Geochemical Perspectives Letters

Ikaite precipitation indicates near-surface occurrence of methane in an Icelandic fjord

A. Hylén[1,2], S. Arndt[3,4], J.P. Balmonte[5], R. Bosman[6], W. Bui[3], L. Chou[3], I. Delbono[7], C. Goossens[1], P.O.J. Hall[8], S. Hidalgo-Martinez[1], R.K. James[3,9], M. Kononets[8,10], P. Ley[1], C. März[11], S.P. Purayil[12], J. Reardon[13], P. Reyniers[14], F. Sales de Freitas[3], L. Verweirder[14], K. Wagner[11], C. Wittig[15], K.R. Hendry[16,17], S.J. van de Velde[1,18,19]

[1]Geobiology Research Group, Department of Biology, University of Antwerp, Universiteitsplein 1, 2610 Wilrijk, Belgium
[2]Aix-Marseille Université, CNRS, IRD, INRAE, CEREGE, Technopôle de l'Arbois-Méditerranée, BP80, 13545 Aix-en-Provence, France
[3]BGeoSys, Department Geosciences, Society and Environment, Université Libre the Bruxelles, Brussels, Belgium
[4]iC3, Department of Geoscience, Arctic University of Norway, Tromso, Norway
[5]Department of Earth and Environmental Sciences, Lehigh University, USA
[6]Institute for Biochemistry and Signal Transduction, University Medical Center Hamburg-Eppendorf, Martinistraße 52, 20246 Hamburg, Germany
[7]ENEA Marine Environment Research Centre, Department for Sustainability, Laboratory of Biodiversity and Ecosystems, 19032 Pozzuolo di Lerici (La Spezia), Italy
[8]Department of Marine Sciences, University of Gothenburg, Box 461, 405 30 Gothenburg, Sweden
[9]Department of Biology, University of Southern Denmark, Odense Denmark
[10]Research consultant, Fredrikas Gård 2, 414 83, Gothenburg, Sweden
[11]Institute for Geosciences, University of Bonn, Kirschallee 1-3, 53115 Bonn, Germany
[12]Operational Directorate Natural Environment, Royal Belgian Institute of Natural Sciences, Brussels, Belgium
[13]External Relations Team, University of Southern Denmark, Odense, Denmark
[14]Department of Geology, Ghent University, Krijgslaan 297, 9000 Ghent, Belgium
[15]Marine Biology Research Group, Ghent University, Ghent, Belgium
[16]British Antarctic Survey, High Cross, Madingley Road, Cambridge, CB3 0ET, UK
[17]Queens' College, University of Cambridge, Silver Street, Cambridge, CB3 9ET, UK
[18]Department of Marine Science, University of Otago, Ōtepoti Dunedin, 9016, Aotearoa New Zealand
[19]Earth Sciences New Zealand, Te Whanganui-a-Tara Wellington, 6021, Aotearoa New Zealand

Supplementary Information

The Supplementary Information includes:

- Methods
- Table S-1
- Figures S-1 to S-3
- Supplementary Information References

The data described in this publication is available in an accompanying dataset (Hylén *et al.,* 2026).

Bottom water conditions and seafloor mapping

Prior to sediment sampling, a CTD (SBE9plus, Sea-Bird Scientific) equipped with an oxygen (O_2) sensor (SBE43, Sea-Bird Scientific) was deployed to record the bottom-water conditions. The bottom water had a salinity of 34.4, a temperature of 4.2 °C, and the O_2 concentration was 287 µmol kg^{-1}.

The hull-mounted Kongsberg EM2040 Dual RX multibeam echosounder onboard RV Belgica was used to acquire bathymetric data. The data were processed using QPS Qimera v2.5.3. This involved time–depth conversion using sound velocity profiles derived from the CTD measurements gathered during the survey, manual noise removal, and gridding the bathymetry at a 5 m resolution.

Sub-bottom data were acquired using a hull-mounted TOPAS PS18 Parametric Sub-Bottom Profiler system operating with a Ricker pulse at 6 kHz. The data were processed in RadExPro v2022.4 using deconvolution, a Butterworth bandpass filter, and amplitude correction. The processed profile has a vertical resolution of about 0.2 m and a maximum penetration depth of about 50 ms two-way travel time. Sub-bottom depths were calculated using a constant sound velocity of 1470 m s^{-1}, which is based on temperature and salinity measurements of the bottom waters at station RF2.

Sediment-water flux incubations

Sediment for sediment-water flux incubations was collected with a NIOZ-type box corer (Ø 50 cm). Three replicate cores were collected approximately 5 m apart and the depth of the collected sediment was approximately 40 cm. The top ~20 cm of sediment in each box core was subsequently sub-cored with a cylindrical incubation chamber (Ø 14.4 cm), which was closed with a gas-tight lid. The cores were then incubated for 19 hours. Concentrations of O_2 were measured continuously using probes (Firesting), and the O_2 fluxes were calculated from the best-fitting slope of concentration versus time over the whole incubation ($R^2 > 0.99$ on average for the incubations). At five time points, discrete water samples of 12 mL and 6 mL

were collected in Exetainers (Labco) for analysis of DIC concentrations and isotopic composition ($\delta^{13}C_{DIC}$), respectively. The DIC samples were analysed within 24 hours, while the $\delta^{13}C_{DIC}$ samples were preserved with 20 µL saturated $HgCl_2$ for later analysis (see below). At the first and last time points, water samples of 50 mL were filtered (0.45 µm, PES) into centrifuge tubes (Falcon) for analysis of alkalinity (A_T) onboard within a few days (see below). The concentrations of A_T and DIC were corrected for dilution during sampling before calculation of the sediment-water fluxes using FLUXER (Hylén and van de Velde, 2025).

Sediment and porewater sampling

Two replicate sediment cores for geochemical profiling were collected with a GEMAX corer (Ø 9 cm) at RF2, or were subcored (Ø 5.9 cm) from the ikaite-site incubation chamber at RF2I. Prior to sediment slicing, the cores were used for microsensor profiling (see below). The cores were sliced at a 0.5-2 cm resolution for determination of solid phase carbon and porewater DIC and A_T. Samples were transferred to centrifuge tubes and were centrifuged at 2800 g for 10 minutes, after which the supernatant was filtered (0.45 µm, PES) into 3 mL Exetainers, which were capped without headspace before storage at 6 °C until analysis within 24 h. The remaining solid phase was freeze-dried and ground in an agate mortar for analysis of carbon and mineralogy.

At station RF2, three more GEMAX cores were collected. Two of the cores were subcored (Ø 5.9 cm) and were sliced under an N_2 atmosphere (Captair Field pyramid, Erlab) at the same resolution as above. The sediment was transferred to centrifuge tubes and Rhizons samplers (MOM; Rhizosphere) were inserted into the sediment to extract porewater for elemental analysis. The porewater was acidified with 15 µL concentrated HNO_3 per mL sample. The remaining solid phase was freeze-dried and stored in aluminum bags under N_2 atmosphere for iron (Fe) and sulfur (S) speciation. The third core was sliced at the same resolution above and was freeze-dried for the determination of porosity and sediment accumulation rates.

Ikaite crystals found at RF2I were immediately frozen. Before further processing, the crystals were rinsed with cold (<2 °C) deionized water.

Microsensor profiling

At station RF2, two replicate sediment cores collected with a GEMAX corer (Ø 9 cm) were subcored (Ø 5.9 cm, 20 cm sediment, ca. 5 cm overlaying water). At station RF2I, two replicate subcores (Ø 4.0 cm, 10 cm sediment) were collected from the sediment used for flux incubations. The latter cores were submerged in bottom water from RF2I in an aquarium. The overlying water of both core types was continuously aerated using an aquarium pump. Microsensor profiling of O_2 (50 µm tip), hydrogen sulfide (H_2S; 100 µm tip) and

pH (200 µm tip) was performed using commercially available microsensors, a multimeter amplifier and a motorized micromanipulator (Unisense A.S., Denmark). Microsensors were calibrated as described previously (Malkin *et al.*, 2014).

Diffusive O_2 fluxes (J_{O2}) were calculated according to Fick's first law from the O_2 porewater profiles:

$$J_{O2} = -\frac{\varphi D_0}{\theta^2} \cdot \frac{\partial C_{O2}}{\partial z} \quad \text{Eq. S-1}$$

where φ is the porosity, D_0 is the molecular diffusion coefficient for O_2 in water, θ is the tortuosity and $\partial C_{O2}/\partial z$ is the linear part of the slope of the O_2 concentration profile over depth. The value of D_0 was calculated as a function of the temperature and salinity using the R package *marelac* (Soetaert *et al.*, 2020), and θ was calculated through the modified Weissberg relation (Boudreau, 1996):

$$\theta^2 = 1 - 2\ln(\varphi) \quad \text{Eq. S-2}$$

Analysis of porewater and incubation water

Concentrations of DIC were determined on board the ship by non-dispersive infrared determination of CO_2 gas (LI-6262/LI-850, LI-COR) after acidification with phosphoric acid. Incubation water samples were analyzed on an Apollo C5L (Apollo SciTech, USA), and porewater was measured using a custom-built DIC analyzer (Nilsson *et al.*, 2019). Repeated measurements of certified reference material (CRM; batch 189 from Dickson Laboratory, Scripps Inst. of Oceanography) were conducted to calibrate the instruments and correct for potential drift in the systems. Repeated measurements of certified reference material (CRM; batch 189 from Dickson Laboratory, Scripps Inst. of Oceanography) were conducted to calibrate the instruments and correct for potential drift in the systems. The analytical precision was 0.2 % relative standard deviation (RSD) for the flux samples and better than 0.6 % RSD for the porewater samples.

The $\delta^{13}C_{DIC}$ values of the samples from the flux incubations were measured on a GasBench II coupled to an isotope ratio mass spectrometer (IRMS; Thermo Delta Plus XP, Thermo Fisher Scientific), and were corrected for isotope fractionation between dissolved and gaseous CO_2. Data were calibrated using the CRMs LSVEC and NBS19 and in-house standards Merck ($\delta^{13}C$ = -9.65 ‰) and Fluka ($\delta^{13}C$ = 2.36 ‰). The precision was <0.08 ‰ (standard deviation; SD) and results are expressed relative to VPDB.

Samples for A_T were analyzed by open-cell potentiometric titration using an automated titrator setup (888 Titrando, Metrohm) according to Dickson *et al.* (2007). The titrator was calibrated using the same CRM as for the DIC concentration analysis and an internal standard (ultrafiltered seawater, 2404 ± 8 µM A_T) was run alongside the samples. The analytical precision was 0.3 % RSD. Due to low volumes (~2 mL), porewater A_T samples were diluted with ultrafiltered seawater to a final volume of 50 mL before analysis. Major and minor

elements in the porewater were measured on an inductive coupled plasma – optical emission spectrometer (ICP-OES; iCAP PRO X Duo, Thermo Fisher). Beryllium and Yttrium were used as internal standards (informative). CRMs CASS-6 and SLEW-4 were spiked and used for quality control. The precision was generally <1 % RSD for most elements and < 3 % for P and Li.

Solid phase carbon analysis

The sedimentary total carbon (TC) concentration and stable isotope carbon composition ($\delta^{13}C_{TC}$) were measured on an elemental analyzer (EA; EA 1110, CE Instruments) connected via a Conflo IV interface (Thermo Fisher Scientific) to an IRMS (Thermo Delta V Advantage, Thermo Fisher Scientific). Data were calibrated using the CRM IAEA-600 and in-house standards leucine ($\delta^{13}C$ = -13.73 ‰, carbon content = 54.72 %) and tuna ($\delta^{13}C$ = -17.96 ‰, carbon content = 45.24 %), calibrated against different CRMs. The precision was <2 % RSD for the carbon content and <0.08 ‰ SD for $\delta^{13}C$, and the $\delta^{13}C$ results are expressed relative to VPDB. The particulate organic carbon (POC) concentration and isotopic composition ($\delta^{13}C_{POC}$) were measured as described above after removal of inorganic carbon from the freeze-dried sediment after treatment with 0.5 M HCl. The sedimentary content of particulate inorganic carbon (PIC) was calculated by subtracting POC from TC. The isotopic compositions of PIC ($\delta^{13}C_{PIC}$) and parts of a freeze-dried ikaite crystal ($\delta^{13}C_{ikaite}$) were measured with the same method as the $\delta^{13}C_{DIC}$ samples.

Mineralogical determination by powder X-ray diffraction

Sediment samples were placed on low-background silicon plates, and mineralogy was identified using X-ray diffraction with an X'Pert Pro diffractometer (PANalytical) fitted with a cobalt tube (λ = 1.79 Å), operating at 40 kV and 40 mA. Samples were analysed from 5º (2θ) to 70º (2θ) with a step size of 0.026º, over a total duration of 2 hours and 7 minutes. The samples were spun at 15 rpm to improve statistics. Phase identification was performed using the software X'Pert HighScore Plus (PANalytical) together with the PDF-2 (Powder Diffraction File 2) database from the ICDD (International Center for Diffraction Data).

Solid phase iron and sulfur speciation

Particulate reactive Fe was extracted by treatment of freeze-dried sediment with 0.5 M HCl under agitation for 1 hour (Laufer *et al.*, 2020). The samples were centrifuged, and the concentrations of Fe(II) and Fe(III) in the supernatant were subsequently determined spectrophotometrically with the ferrozine method (Viollier *et al.*, 2000).

The sedimentary contents of acid reducible sulfides (AVS, e.g. FeS) and chromium reducible sulfides (CRS, e.g., FeS_2 and S_0) were determined through a two-step sequential extraction (Kallmeyer *et al.*, 2004). First, the AVS fraction was obtained by adding a 6 M HCl solution to freeze-dried sediment in a reaction flask. Over 40 minutes, the H_2S was stripped from the solution to a 5 % zinc acetate solution trap using N_2 as a carrier gas. The zinc acetate trap was subsequently replaced before addition of N,N di-methyl formamide (DMF) and a reduced chromium solution to the reaction flask for a further 40 minutes of extraction. The S in the traps was measured spectrophotometrically with the Cline method (Cline, 1969).

Porosity and sediment accumulation rates

The porosity of the sediment was determined from the weight loss after freeze drying, corrected for the salt content of the porewater. Radiometric analyses were performed by gamma spectrometry. Each sample was counted for 1-3 days on high-purity germanium detectors with carbon fiber windows for the detection of low-energy gamma rays. At a ^{60}Co gamma emission energy of 1.33 MeV, the detector efficiency was 60% with a resolution of 2.2 keV. Calibrations for ^{210}Pb and ^{226}Ra, ^{228}Th and ^{228}Ra were performed using an internal standard derived from the CANMET (Canadian Centre for Mineral and Energy Technology) reference standard DL1a and IAEA (International Atomic Energy Agency) reference standard RGTH1. The calibration for ^{137}Cs was performed using the multi-elemental reference standard QCYA48 from Eckert & Ziegler Analytics. Quality controls were routinely performed by analyzing the standard reference material IAEA-385. To evaluate the sediment accumulation rate (SAR), a numerical model that calculates radionuclide profiles in a sediment core affected by diffusion in a surficial layer was applied to the data (Buffoni *et al.*, 2020). The vertical profiles of ^{210}Pb excess, ^{137}Cs and ^{228}Th excess were simultaneously fitted to determine the best estimate of SAR.

Single-crystal X-ray diffraction

Frozen ikaite crystals were broken apart at 4 °C and attached to SPINE mounts and stored on ice. Samples were cryo-cooled under a N_2 cryostream (CryoJet XL, Oxford Instruments) set to 110 K. Manual alignment was performed along clearly discernible crystal edges to minimize overlapping lattices. Data collection was carried out on a XtaLAB Synergy-R diffractometer with a high-flux rotating anode (Rigaku). Data reduction was done in CrystalisPro and data was indexed and integrated into a = 8.760 Å, b = 8.305 Å, c = 11.000 Å, β = 110.477, space group C2/c, Rint = 0.099. The space group and unit cell contents were confirmed in ShelXT.

Calculation of contributions from different sources to the DIC flux

The contribution of carbonate dissolution to the DIC flux was calculated using the Keeling plot method (Keeling, 1958; Pataki *et al.*, 2003). The isotopic composition of the DIC being released from the sediment ($\delta^{13}C_{Sed}$) can be obtained by calculating the intercept of a regression of 1/DIC versus its $\delta^{13}C$ values ($\delta^{13}C_{DIC}$). We assume that DIC released from the sediment stems from either degradation of organic matter or dissolution of carbonates, so that:

$$1 = f_{POC} + f_{PIC} \quad \text{Eq. S-3}$$

where f_{POC} and f_{PIC} are the fractions of DIC produced through organic matter degradation and carbonate dissolution, respectively. Conservation of mass gives that:

$$\delta^{13}C_{Sed} = f_{POC} \cdot \delta^{13}C_{POC} + f_{PIC} \cdot \delta^{13}C_{PIC} \quad \text{Eq. S-4}$$

where $\delta^{13}C_{POC}$ and $\delta^{13}C_{PIC}$ are the average carbon isotope ratios of the solid phase organic and inorganic carbon, respectively, in the top 5 cm of sediment. The contribution from carbonate dissolution to the total DIC flux (f_{PIC}) can thereby be calculated by combining Eq. S-3 and Eq. S-4:

$$f_{PIC} = \frac{\delta^{13}C_{Sed} - \delta^{13}C_{POC}}{\delta^{13}C_{PIC} - \delta^{13}C_{POC}} \quad \text{Eq. S-5}$$

Data used for the calculations and the resulting f_{PIC} values are presented in Table S-1.

Supplementary Tables

Table S-1 Data used for calculating the contribution from carbonate dissolution to the sedimentary DIC flux (fPIC) and the resulting fPIC for each incubation chamber. The numbers for $\delta^{13}C_{POC}$ and $\delta^{13}C_{PIC}$ are average values for the top 5 cm of sediment at stations RF2 (chambers 1 and 3) and RF2I (chamber 2), and the uncertainty is the standard deviation of the measurements. The uncertainty for $\delta^{13}C_{Sed}$ is the standard error of the intercept on the Keeling plot.

Incubation chamber (station)	$\delta^{13}C_{Sed}$ (‰)	$\delta^{13}C_{POC}$ (‰)	$\delta^{13}C_{PIC}$ (‰)	f_{PIC}
1 (RF2)	-7.85 ± 2.32	-22.35 ± 0.08	-0.50 ± 0.26	0.66
3 (RF2)	-14.55 ± 2.91	-22.35 ± 0.08	-0.50 ± 0.26	0.36
2 (RF2I)	-22.72 ± 0.72	-22.22 ± 0.08	-0.71 ± 0.26	-0.02

Supplementary Figures

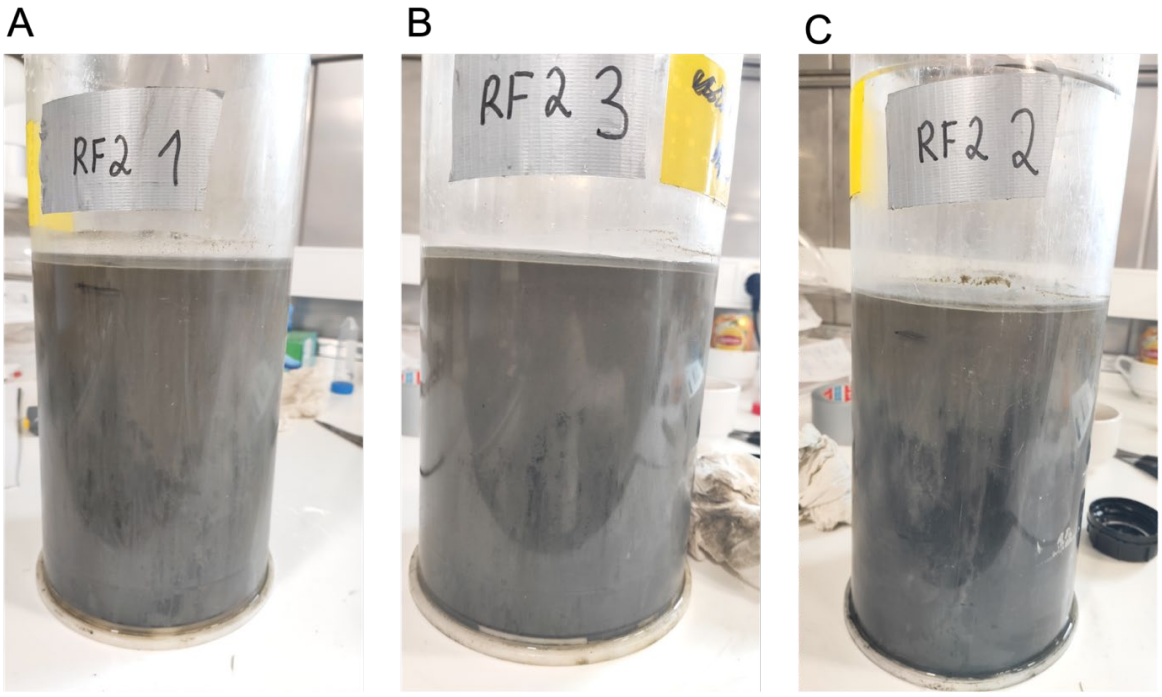

Figure S-1 Sediment after the end of the incubation. A and B show cores from RF2, C shows the core from RF2I.

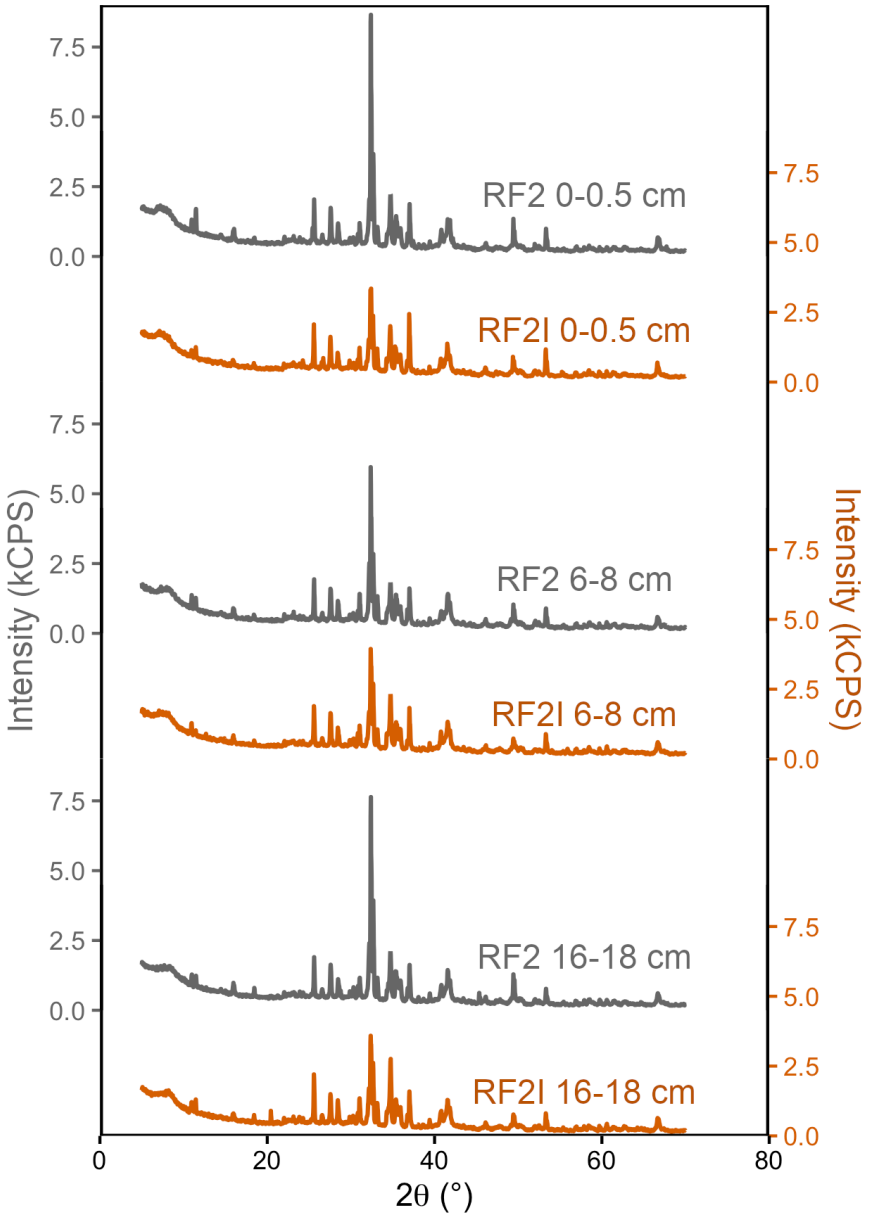

Figure S-2 XRD spectra from 0-0.5, 6-8, and 16-18 cm sediment depths at stations RF2 (grey) and RF2I (orange). The major phases identified were consistent across all samples and included andesine, diopside, chabazite, quartz, calcite, and halite (precipitated during sample drying). Note that the samples were handled and stored under oxic conditions, meaning oxygen-sensitive minerals may have been reoxidised.

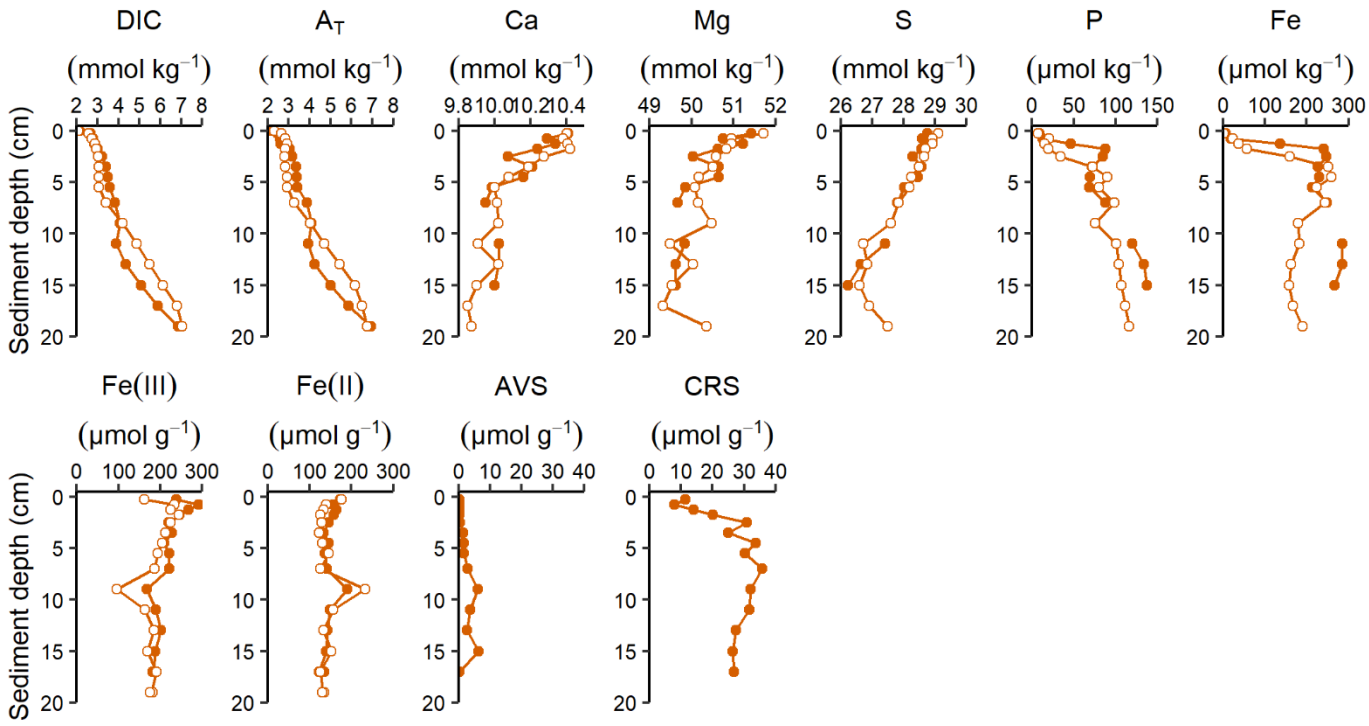

Figure S-3 Porewater profiles (top) and solid phase composition (bottom) at station RF2. Ca, Mg, S, P and Fe were measured by ICP-OES and are assumed to represent Ca^{2+}, Mg^{2+}, SO_4^{2-}, PO_4^{3-} and Fe^{2+}. Fe(III) = oxidized iron, Fe(II) = reduced iron, AVS = acid volatile sulphides, CRS = chromium reducible sulphides.

Supplementary Information References

Boudreau, B.P. (1996) The diffusive tortuosity of fine-grained unlithified sediments. *Geochimica et Cosmochimica Acta* 60, 3139–3142. https://doi.org/10.1016/0016-7037(96)00158-5

Buffoni, G., Schirone, A., Delfanti, R. (2020) A numerical investigation for dating 210Pbex and 137Cs vertical profiles in a coastal area: The Eastern Ligurian Sea, Italy. *Journal of Environmental Radioactivity* 212, 106122. https://doi.org/10.1016/j.jenvrad.2019.106122

Cline, J.D. (1969) Spectrophotometric determination of hydrogen sulfide. *Limnology and Oceanography* 14, 454–458. https://doi.org/10.4319/lo.1969.14.3.0454

Dickson, A.G., Sabine, C.L., Christian, J.R. (Eds.) (2007) *Guide to best practices for ocean CO_2 measurements*. PICES Special Publication 3, 191 pp.

Hylén, A., van de Velde, S. (2025) FLUXER. Zenodo. https://doi.org/10.5281/ZENODO.14758688

Hylén, A., Arndt, S., Balmonte, J.P., Bosman, R., Bui, W., Chou, L., Delbono, I., Goossens, C., Hall, P., Hidalgo Martinez, S., James, R.K., Kononets, M., Ley, P., März, C., Puthan Purayil, S., Reardon, J., Reyniers, P., Sales de Freitas, F., Verweirder, L., Wagner, K., Wittig, C., Hendry, K., van de Velde, S. (2026) Dataset for Ikaite precipitation indicates near-surface occurrence of methane in an Icelandic fjord. *Zenodo*. https://doi.org/10.5281/ZENODO.20053641

Kallmeyer, J., Ferdelman, T.G., Weber, A., Fossing, H., Jørgensen, B.B. (2004) A cold chromium distillation procedure for radiolabeled sulfide applied to sulfate reduction measurements. *Limnology and Oceanography: Methods* 2, 171–180. https://doi.org/10.4319/lom.2004.2.171

Keeling, C.D. (1958) The concentration and isotopic abundances of atmospheric carbon dioxide in rural areas. *Geochimica et Cosmochimica Acta* 13, 322–334. https://doi.org/10.1016/0016-7037(58)90033-4

Laufer, K., Michaud, A.B., Røy, H., Jørgensen, B.B. (2020) Reactivity of Iron Minerals in the Seabed Toward Microbial Reduction – A Comparison of Different Extraction Techniques. *Geomicrobiology Journal* 37, 170–189. https://doi.org/10.1080/01490451.2019.1679291

Malkin, S.Y., Rao, A.M., Seitaj, D., Vasquez-Cardenas, D., Zetsche, E.-M., Hidalgo-Martinez, S., Boschker, H.T., Meysman, F.J. (2014) Natural occurrence of microbial sulphur oxidation by long-range electron transport in the seafloor. *The ISME Journal* 8, 1843–1854. https://doi.org/10.1038/ismej.2014.41

Nilsson, M.M., Kononets, M.Y., Ekeroth, N., Viktorsson, L., Hylén, A., Sommer, S., Pfannkuche, O., Almroth-Rosell, E., Atamanchuk, D., Andersson, H.J., Roos, P., Tengberg, A., Hall, P.O.J. (2019) Organic carbon recycling in Baltic Sea sediments – An integrated estimate on the system scale based on in situ measurements. *Marine Chemistry* 209, 81–93. https://doi.org/10.1016/j.marchem.2018.11.004

Pataki, D.E., Ehleringer, J.R., Flanagan, L.B., Yakir, D., Bowling, D.R., Still, C.J., Buchmann, N., Kaplan, J.O., Berry, J.A. (2003) The application and interpretation of Keeling plots in terrestrial carbon cycle research. *Global Biogeochemical Cycles* 17. https://doi.org/10.1029/2001GB001850.

Soetaert, K., Petzoldt, T., Meysman, F.J.R., Meire, L. (2020) "marelac" R package, v. 2.1.10

Viollier, E., Inglett, P.W., Hunter, K., Roychoudhury, A.N., Van Cappellen, P. (2000) The ferrozine method revisited: Fe(II)/Fe(III) determination in natural waters. *Applied Geochemistry* 15, 785–790. https://doi.org/10.1016/S0883-2927(99)00097-9